Neuron-to-astrocyte signaling is central to the dynamic control of brain microcirculation

Micaela Zonta[1], María Cecilia Angulo[1,2], Sara Gobbo[1], Bernhard Rosengarten[3], Konstantin-A. Hossmann[3], Tullio Pozzan[1] and Giorgio Carmignoto[1]

[1] *Istituto CNR di Neuroscienze and Dipartimento di Scienze Biomediche Sperimentali, Università di Padova, viale G. Colombo 3, 35121 Padova, Italy*

[2] *Centro Internacional de Física, Ed. Manuel Ancízar, Ciudad Universitaria, Bogotá, Colombia*

[3] *Department of Experimental Neurology, Max Planck Institute for Neurological Research, Gleueler Strasse 50, 50931 Cologne, Germany*

The first two authors contributed equally to this work.

Correspondence should be addressed to G.C. (gcarmi@bio.unipd.it)

Published online 25 November 2002; corrected 9 December 2002 (details online); doi:10.1038/nn980

The cellular mechanisms underlying functional hyperemia—the coupling of neuronal activation to cerebral blood vessel responses—are not yet known. Here we show in rat cortical slices that the dilation of arterioles triggered by neuronal activity is dependent on glutamate-mediated $[Ca^{2+}]_i$ oscillations in astrocytes. Inhibition of these Ca^{2+} responses resulted in the impairment of activity-dependent vasodilation, whereas selective activation—by patch pipette—of single astrocytes that were in contact with arterioles triggered vessel relaxation. We also found that a cyclooxygenase product is centrally involved in this astrocyte-mediated control of arterioles. *In vivo* blockade of glutamate-mediated $[Ca^{2+}]_i$ elevations in astrocytes reduced the blood flow increase in the somatosensory cortex during contralateral forepaw stimulation. Taken together, our findings show that neuron-to-astrocyte signaling is a key mechanism in functional hyperemia.

© 2003 Nature Publishing Group http://www.nature.com/natureneuroscience

A remarkable feature of the brain is its high degree of functional specialization. When neurons in a specific brain region are highly activated, blood flow increases in a temporally and spatially coordinated manner. Functional hyperemia, the tight coupling between neuronal activity and blood flow, is fundamental to brain function and was first described by Sherrington more than a century ago[1]. Although functional hyperemia is increasingly used in basic and clinical neurosciences, especially in brain imaging techniques, its signaling pathway remains elusive.

The extensive innervation of cerebral blood vessels suggests that neurons directly control the local changes in cerebral blood flow (CBF) associated with neuronal activity[2–6], but this idea is still up for debate. Alternative explanations have been proposed, such as local acidosis or changes in tissue concentration of adenosine and lactate, but no firm experimental evidence has yet been provided in their support[7]. Here we propose that local arteriole dilation in response to high neuronal activity largely depends on the activation of astrocytes by locally released neurotransmitters. Our hypothesis originates from three observations: (i) astrocyte processes are in close contact with both neuronal synapses[8–10] and cerebral arterioles[5,9], (ii) astrocytes are accurate sensors of neuronal activity and respond to the synaptic release of glutamate with oscillations in the intracellular calcium concentration ($[Ca^{2+}]_i$)[11–13] and (iii) glutamate-mediated $[Ca^{2+}]_i$ elevations in astrocytes trigger the release of vasoactive compounds such as eicosanoids[14,15]. The findings reported here point to a crucial role for astrocytes in the dynamic control of brain microcirculation.

Results

Afferent stimulation triggers dilation of arterioles

To investigate the mechanism(s) underlying neuronal–vascular coupling, we used acute cortical slices as an experimental model. Blood vessels from this preparation retain responsiveness to vasoactive factors[16–18]. Dilating agents such as prostaglandin E_2 (PGE_2) and prostacyclin induced relaxation of cerebral vessels ($14.9 \pm 3.10\%$, $n = 12$ and $11.6 \pm 9.24\%$, $n = 2$, respectively), whereas agents such as $PGF_{2\alpha}$ and the nitric oxide synthase (NOS) inhibitor N-nitro-L-arginine methyl ester (L-NAME) induced vasoconstriction ($-22.3 \pm 3.33\%$, $n = 3$ and $-32.0 \pm 4.22\%$, $n = 21$, respectively). After stimulation of neuronal afferents through an extracellular electrode placed intracortically, arterioles showed a transient relaxation (**Fig. 1a** and **b**). The kinetics of the arterioles' diameter changes after two successive stimulations are also shown (**Fig. 1c**). The effects of neuronal afferent stimulation were studied in 16 arterioles, and in 8 of these, we found significant dilation (mean, $14.8 \pm 3.13\%$, $n = 8$). In all experiments, the intensity of the applied stimulus was adjusted to evoke large-amplitude excitatory postsynaptic responses from neurons positioned between the electrode and the arteriole (**Fig. 2c**, inset).

Astrocyte endfeet respond to afferent stimulation

The stimulation of neuronal afferents that triggered vasodilation also triggered $[Ca^{2+}]_i$ elevations in astrocyte endfeet surrounding arterioles. In the example reported (**Fig. 1d**), the first stimu-

© 2003 Nature Publishing Group http://www.nature.com/natureneuroscience

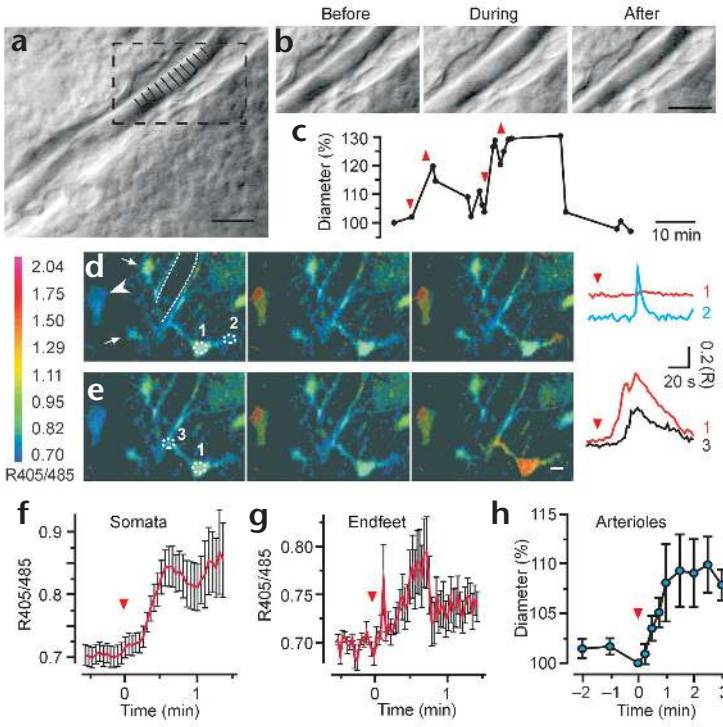

Fig. 1. Neuronal afferent stimulation mediates dilation of cerebral arterioles and $[Ca^{2+}]_i$ elevations in astrocyte somata and endfeet. (**a**) A typical arteriole and associated structures from a cortical slice. Note similarity to vascular myocytes. Boxed sector was measured at 11 places, as indicated by parallel black lines. (**b**) Images of this sector before, during and after afferent stimulation applied for 4 min through an intracortical electrode. According to Poiseuille's law, an increase in vessel diameter *in vivo* similar to that which we observed in our slice preparation (about 20%) would double the blood flow in this arteriole. Scale bars (**a**, **b**), 10 μm. (**c**) Kinetics of diameter changes in the arteriole sector. In this and all subsequent figures, down and up triangles indicate the onset and the offset of stimulation, respectively. (**d**, **e**) Sequences of pseudocolor images of an arteriole (dashed white line) from a different slice loaded with Indo-1, showing the $[Ca^{2+}]_i$ changes that occurred in an astrocyte contacting the arteriole upon a first (**d**) and a second (**e**) neuronal stimulation (each afferent stimulation, 4 min). Kinetics of $[Ca^{2+}]_i$ changes at soma (1), distal process (2) and endfoot (3) of this astrocyte are reported on the right of each sequence. Stimulation also triggered $[Ca^{2+}]_i$ elevations in a pyramidal neuron (white arrowhead). Two other astrocytes in contact with the same arteriole (arrows) also showed $[Ca^{2+}]_i$ elevations upon afferent stimulation (**Supplementary Fig. 1** online). R corresponds to the R405/485 ratio. Acquisition rate, 2 s. Scale bar, 10 μm. (**f**, **g**) Kinetics of $[Ca^{2+}]_i$ elevations in astrocytes obtained by averaging the R405/485 changes measured in the soma (**f**, $n = 23$) and endfeet (**g**, $n = 13$) of each responsive cell. Owing to inadequate Indo-1 loading in the endfeet and to their small size, the measurements of the change in the fluorescent signal in endfeet are relatively accurate and could not be ensured for all responsive astrocytes. As such, the trace of R405/485 change in endfeet (**g**) is more noisy than in the somata, and the values of the R405/485 increase are lower (see also **Fig. 3j**). (**h**) Time course of the dilation of arterioles obtained by averaging the diameter change upon each episode of stimulation ($n = 16$).

lation triggered a $[Ca^{2+}]_i$ increase that was restricted to the distal astrocyte process. In response to the second stimulation, however, the soma and endfoot that were in contact with the arteriole were also involved (**Fig. 1e**). Neuronal activity-dependent $[Ca^{2+}]_i$ elevations were observed in 23 of 31 (74.2%) astrocytes examined within a few seconds after the onset of the stimulation, reaching a peak at somata and endfeet after an average of 32 ± 4.6 s ($n = 23$) and 33 ± 7.5 s ($n = 13$), respectively. Notably, the average onset of dilation occurred 34 ± 6.8 s after stimulation, suggesting a possible link between the astrocyte response and the onset of dilation. For technical reasons, we could not simultaneously monitor the $[Ca^{2+}]_i$ change in astrocytes and the arteriole dilation (Methods). We thus analyzed the time course of these two events in separate experiments. The analysis of the timings for $[Ca^{2+}]_i$ elevations in astrocyte soma (**Fig. 1f**) and endfeet (**Fig. 1g**) and for arteriole dilation (**Fig. 1h**) showed that the two events occurred in a temporally correlated manner.

mGluR antagonists reduce dilation of arterioles

In the next series of experiments, we stimulated neuronal afferents in the absence or in the presence of LY367385 and MPEP, antagonists of subtypes 1 and 5, respectively, of group I metabotropic glutamate receptors (mGluRs)[19]. These mGluRs are known to mediate the $[Ca^{2+}]_i$ increase of astrocytes in response to synaptically released glutamate[11,12]. If $[Ca^{2+}]_i$ elevations triggered in astrocytes by neuronal activity are crucial for neuronal–vascular coupling, their specific block should hamper arteriole dilation induced by afferent

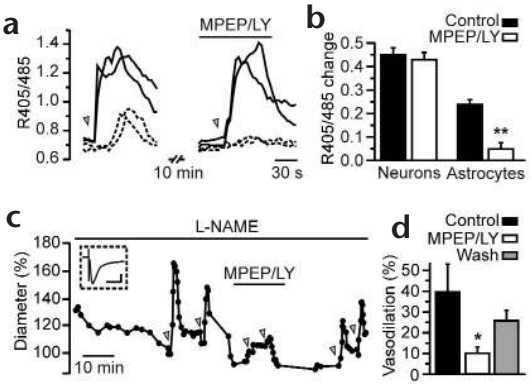

Fig. 2. The blockade of $[Ca^{2+}]_i$ elevations in astrocytes by mGluR antagonists impairs neuronal activity–dependent vasodilation. (**a**) Kinetics of $[Ca^{2+}]_i$ changes induced by afferent stimulation in two neurons (solid lines) and two astrocytes (dashed lines) from the neocortex, in the absence or presence of 50 μM MPEP and 100 μM LY367385. (**b**) Mean values of R405/485 change in neurons ($n = 62$) and astrocytes ($n = 11$) upon neuronal stimulation (**$P < 0.001$). (**c**) Kinetics of the diameter change of an arteriole upon successive afferent stimulation applied in the absence, presence or after washout of MPEP/LY. Inset, evoked postsynaptic response from a patched neuron voltage clamped at –60 mV (scale bars, 25 ms and 250 pA). In both types of experiment described in (**a**) and (**c**), the 1 min protocol of afferent stimulation was applied. For clarity, only the onsets of stimulation (down triangles) are marked. (**d**) Mean values of neuronal activity–dependent vasodilation, calculated for dilated vessels under different experimental conditions (*$P < 0.05$ compared with mean control values obtained before MPEP/LY and after washout).

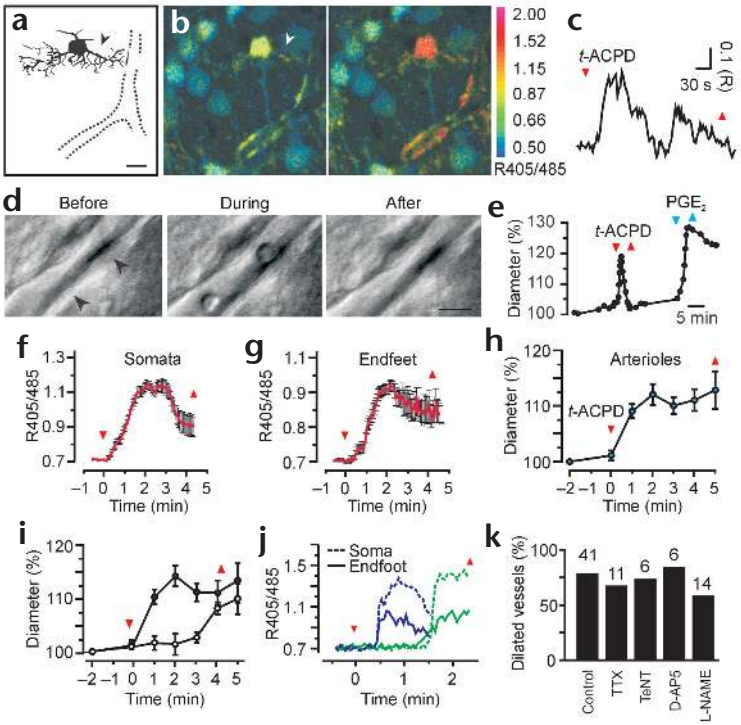

Fig. 3. Stimulation with *t*-ACPD induces $[Ca^{2+}]_i$ increases in astrocytes and dilation of cerebral arterioles. (**a**) Reconstruction from 20 confocal microscope images at different focal planes of an Indo-1-loaded astrocyte contacting an arteriole (dashed line). The arrowhead indicates the astrocyte process impinging on the arteriole. Scale bar, 10 μm. (**b**, **c**) Pseudocolour images (**b**) and kinetics (**c**) of $[Ca^{2+}]_i$ oscillations of the astrocyte endfoot upon 50 μM *t*-ACPD application. Acquisition rate, 3 s. (**d**) Images of an arteriole before (basal condition), during and after *t*-ACPD stimulation. Scale bar, 10 μm. (**e**) Kinetics of diameter changes in the arteriole sector, indicated by the black arrowheads in (**d**), induced by 100 μM *t*-ACPD and 20 μM PGE_2. (**f**, **g**) Mean kinetics of R405/485 changes measured at the astrocyte somata (**f**, $n = 81$) and endfeet (**g**, $n = 57$) after *t*-ACPD. (**h**) Time course of the vasodilation triggered by *t*-ACPD. Reported here are arterioles that were monitored by an acquisition rate of 1 min or less. (**i**) Mean values ± s.e.m. of the rapid (closed circle, $n = 20$) or delayed (open circle, $n = 6$) diameter change in arterioles. We grouped together the arterioles that dilated within 1 min and those that dilated after 3 min of *t*-ACPD. (**j**) Kinetics of the rapid and delayed $[Ca^{2+}]_i$ change measured at the soma or endfeet of two representative astrocytes in response to *t*-ACPD. (**k**) Percentage of arterioles that showed significant dilation upon *t*-ACPD application under different experimental conditions. Numbers below bars indicate the number of analyzed arterioles in each type of experiment. As compared to controls, no significant differences were observed when *t*-ACPD was applied in the presence of TTX, TeNT, D-AP5 or L-NAME.

stimulation. In confocal microscope experiments, we found that $[Ca^{2+}]_i$ elevations evoked in astrocytes by afferent stimulation were impaired by mGluR antagonists, whereas those in neurons were unaffected (**Fig. 2a**). The mean amplitude of the response from astrocytes, but not that from neurons, was drastically reduced in the presence of MPEP and LY367385 (MPEP/LY, $P < 0.001$, **Fig. 2b**). These results allowed us to investigate more directly the involvement of astrocytes in neuronal activity-dependent vasodilation. In preconstricted arterioles, the action of vasodilating agents is enhanced[17], so we perfused slices with the NOS inhibitor L-NAME[7,17]. Indeed, by inhibiting the tonic release of NO, L-NAME (100 μM) induced a progressive vasoconstriction that began after 10–15 minutes, reached a peak after 40–50 minutes (mean constriction, –32.0 ± 4.22%; $n = 21$) and remained stable thereafter. Afferent stimulation was thus performed after slice perfusion with L-NAME for a fixed period of 50 minutes. In the arterioles examined ($n = 4$), afferent stimulation triggered a dilation that was significantly higher than in control slices (39.9 ± 13.09%, $n = 4$ versus 14.8 ± 3.13%, $n = 8$; $P < 0.025$), most likely due to the preconstriction of arterioles that increases the range of their possible relaxation. Arteriole dilation was severely impaired when a second episode of stimulation was given in the presence of the mGluR antagonists MPEP (50 μM) and LY367385 (100 μM; **Fig. 2c**; $n = 2$). See also **Supplementary Movie 1a** and **b** and **Supplementary Fig. 2** online. After the removal of the antagonists, a third stimulation was given, and vasodilation was seen again (**Fig. 2c**; $n = 2$). The effect of the mGluR antagonists was confirmed when the first stimulation was given in the presence of MPEP and LY367385 and the second after their removal ($n = 3$). The mean dilating response in the presence of the mGluR antagonists (10.0 ± 3.36%, $n = 5$) was significantly lower than that measured both in their absence (39.9 ± 13.09%, $n = 4$; $P < 0.05$) and after their washout (25.7 ± 7.32%, $n = 5$; $P < 0.025$; **Fig. 2d**). The effect of the mGluR antagonists on neuronal activity-dependent vasodilation could not be attributed to a direct effect on vessels because in their presence, arterioles still showed a marked dilation in response to an increase in the CO_2 pressure in the perfusate, which lowered the pH to 6.1 (mean dilation 20.8 ± 7.32%, $n = 3$).

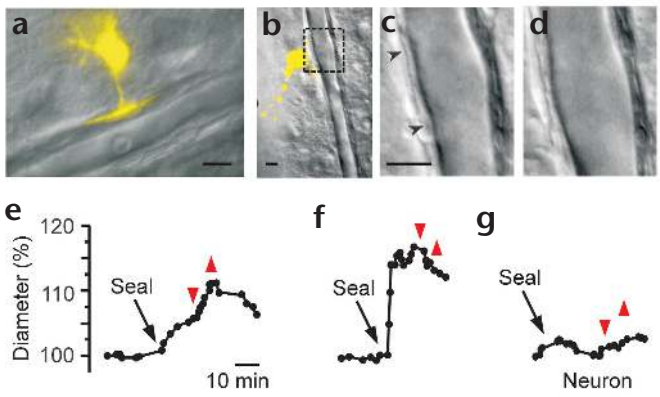

Fig. 4. Direct stimulation of an individual astrocyte results in arteriole dilation. (**a**, **b**) Fluorescent (Lucifer yellow) images of two perivascular astrocytes superimposed to DIC images of the nearby arterioles. Note the processes in contact with the arteriole. (**c**, **d**) Magnification of the arteriole sector delimited by the dashed line box in (**b**), before and after astrocyte stimulation. Black arrowheads delimit the analyzed sector. Scale bars, 10 μm. (**e**) Kinetics of the diameter changes from the analyzed sector. (**f**) Kinetics of the diameter changes from a different arteriole that showed the maximal dilation after seal formation in a nearby astrocyte. (**g**) Kinetics of diameter changes from an arteriole upon seal formation and delivery of depolarizing stimuli to a nearby neuron.

© 2003 Nature Publishing Group http://www.nature.com/natureneuroscience

© 2003 Nature Publishing Group http://www.nature.com/natureneuroscience

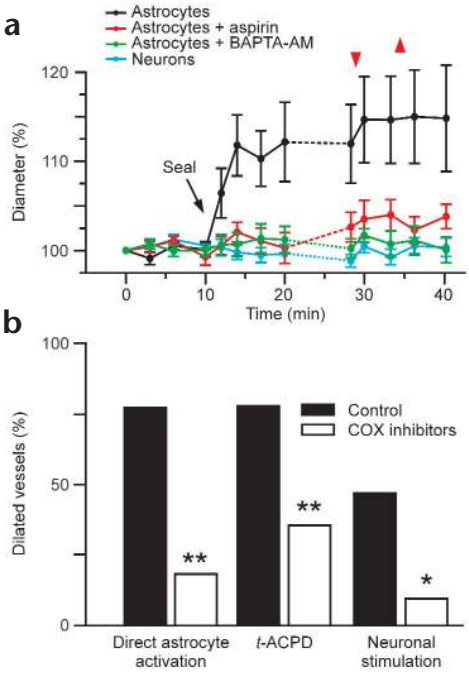

Fig. 5. The action of astrocytes depends mainly on a COX product. (**a**) Time-course plots of diameter changes in the arterioles upon direct stimulation of nearby astrocytes in control slices (n = 13, black line) and in slices preincubated with either 50 μM aspirin (n = 11, red line) or 50 μM BAPTA-AM (n = 9, green line), as well as in the arterioles upon seal formation (n = 8) and delivery of depolarizing stimuli (n = 6) to nearby neurons (blue line). The time interval between the end of image acquisition after the formation of the seal and the application of the intracellular stimulus varied from 0–10 min (dashed lines). Values are given as mean ± s.e.m. expressed as percentage of baseline. The mean basal values were significantly different ($P < 0.05$) from the mean values of the arteriole diameter change after astrocyte stimulation at all time points. In contrast, these mean values were not significantly changed after stimulation of astrocytes from slices incubated with aspirin or BAPTA-AM, or after stimulation of neurons. (**b**) Summary bar graph reporting the percentage of arterioles showing significant dilation upon direct stimulation of astrocytes, application of *t*-ACPD and afferent stimulation in the absence (control) or presence of COX inhibitors. (**$P < 0.01$; *$P < 0.05$).

Role of NO in dilation of cortical arterioles

The release from neurons of the vasodilator NO after NMDA receptor (NMDAR) activation may be one of the main signals that control vascular tone[20–23]. Our results in slices perfused with L-NAME indicate that the inhibition of NO synthesis does not impair the ability of afferent stimulation to evoke vasodilation. To further investigate the possible role of neuronal signals associated with NMDAR activation, we perfused slices with the NMDAR blocker D-AP5 (100 μM). Under these conditions, afferent stimulation triggered dilation in 41.6% of arterioles examined (5 of 12), which was not significantly different (n.s.) from controls (50%; 8 of 16); mean dilation was 11.3 ± 1.59% (control, 14.8 ± 3.13%; n.s.), indicating that neuronal activity-dependent vasodilation was not affected by NMDAR inhibition.

t-ACPD induces dilation of arterioles

We next investigated whether specific stimulation of mGluRs resulted in vasodilation. The mGluR agonist *t*-ACPD elicited $[Ca^{2+}]_i$ elevations in both astrocyte somata and processes (**Fig. 3a–c**). *t*-ACPD also induced a powerful vasodilation (**Fig. 3d** and **e**; also **Supplementary Movie 2** and **Supplementary Fig. 3** online) that could be observed in the same region upon stimulation with the vasodilator PGE_2. Significant dilation was found in 32 of 41 (78%) arterioles examined (mean dilation, 18.3 ± 1.86%; n = 32) and, in most arterioles, it was rapidly triggered upon *t*-ACPD application (**Fig. 3i**). The analysis of the timings for $[Ca^{2+}]_i$ elevations in astrocytes (**Fig. 3f** and **g**) and for vasodilation (**Fig. 3h**) after *t*-ACPD revealed that the two events occurred in a temporally correlated manner. The mean peak of $[Ca^{2+}]_i$ elevations at the astrocyte somata and endfeet occurred 79 ± 2.9 s (n = 81) and 78 ± 3.5 s (n = 57) after *t*-ACPD, whereas vasodilation started at 83 ± 11.8 s (n = 26). Compared with that triggered by afferent stimulation, the calcium rise in astrocytes that was triggered by *t*-ACPD occurred with a more variable delay. Some astrocytes and their endfeet showed $[Ca^{2+}]_i$ elevations within 20–30 s after *t*-ACPD; others responded with more delay (**Fig. 3j**). The onset of arteriole dilation was also variable, occurring in some arterioles within the first minute of stimulation and in others after three minutes (**Fig. 3i**). Differences in *t*-ACPD penetration in the various experiments as well as in position and deepness of arterioles and astrocytes under study represent the most plausible explanation for the variable timing of the response.

Although *t*-ACPD is a powerful stimulus for astrocytes, it can also induce $[Ca^{2+}]_i$ increases in neurons[24]. Activation of neuronal mGluRs is also known to potentiate the NMDAR[25], and this may, in turn, potentiate the release of NO from neurons[21]. To test this possibility, we perfused slices with either the NMDAR antagonist D-AP5 (100 μM) or L-NAME (100 μM). In the presence of D-AP5, *t*-ACPD triggered dilation in 83.3% of the arterioles (5 of 6, mean dilation 21.7 ± 10.46%; **Fig. 3k**). After L-NAME perfusion, 57.1% of the arterioles were responsive

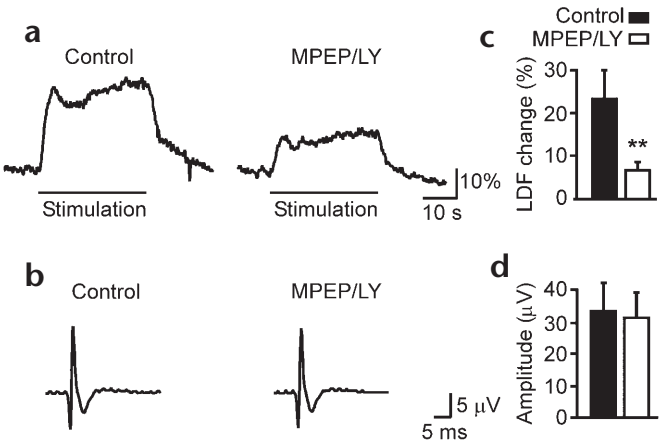

Fig. 6. The mGluR antagonists MPEP and LY367385 reduce the hyperemic response in the somatosensory cortex *in vivo*. (**a**, **b**) Representative recordings of the CBF increase in the somatosensory cortex (**a**) and cortical evoked potentials (**b**) from a chloralose-anaesthetized rat during electrical stimulation of contralateral forepaw. Measurements were carried out before (control) and after the intravenous injection of MPEP and LY367385. (**c**, **d**) Mean values (mean ± s.e.m.) of LDF signal changes (**c**) and evoked potentials (**d**). Note the significant reduction by MPEP and LY367385 of the integrated flow responses but not of evoked potentials (**$P < 0.01$). The resting LDF signal was unchanged (1.3 ± 0.6%, n.s.; data not shown).

© 2003 Nature Publishing Group http://www.nature.com/natureneuroscience

to *t*-ACPD (n.s., 8 of 14 versus 32 of 41 in controls; mean dilation, 26.5 ± 9.59%). In the presence of tetrodotoxin (TTX), which blocks neuronal transmission, or tetanus toxin (TeNT), which inhibits neurotransmitter release[12,26], the percentage of vessels responsive to *t*-ACPD (TTX, 8 of 11, 72.7%; TeNT, 4 of 6, 66.7%) and their degree of relaxation (mean dilation, 18.7 ± 2.92% and 13.9 ± 5.4% in TTX and TeNT, respectively) were not significantly changed as compared to controls (**Fig. 3k**).

Direct astrocyte stimulation triggers vasodilation

Can astrocytes control vascular tone without the contribution of factors released from activated neurons? We used a patch pipette to selectively evoke $[Ca^{2+}]_i$ elevations in astrocytes located near arterioles (within 10–20 μm). Individual astrocytes were stimulated with a patch pipette containing Lucifer yellow, first mechanically by touching the cell membrane during the formation of the seal, and then by applying intracellular depolarizing current pulses[13,27]. Most astrocytes in close proximity to arterioles had processes that contacted the vessel wall (**Fig. 4a**). In 10 of 13 arterioles, astrocyte stimulation resulted in the dilation of the nearby arteriole (mean dilation, 20.3 ± 5.79%, $n = 10$). The direct stimulation of an astrocyte triggered the dilation of the arteriole region that was in contact with that astrocyte's process (**Fig. 4c** and **d**). The time course of the diameter change in this arteriole is also reported (**Fig. 4e**). In all astrocytes, seal formation was sufficient to trigger vasodilation (16.7 ± 4.50%), and in four cases, intracellular stimulation caused a further dilation of 8.4 ± 3.29% (**Fig. 4e**). In most astrocytes, the seal rapidly elicited such a powerful dilation that the subsequent stimulation was ineffective (**Fig. 4f**). The time course of the mean change in diameter evoked by direct astrocyte stimulation in all arterioles is reported ($n = 13$, **Fig. 5a**). In slices preincubated with BAPTA-AM to chelate $[Ca^{2+}]_i$ elevations in cortical cells, the direct stimulation of astrocytes did not elicit arteriole dilation ($n = 9$; **Fig. 5a**, green line). Moreover, a mechanical stimulus to the vessel wall applied with the pipette tip always triggered a powerful vasoconstriction ($n = 7$). To further control for the specificity of the astrocyte effects, we directly stimulated individual neurons located within 10–20 μm from arterioles by either seal formation ($n = 8$) and application of depolarizing current pulses ($n = 6$). No effects were observed on the vessels (**Figs. 4g** and **5a**, blue line). We also examined the possibility that the activation of astrocytes during seal formation leads to a potassium efflux from these cells through Ca^{2+}-activated K^+ channels that depolarizes nearby neurons and thus evokes a neuron-mediated vasodilation. By recording from neurons in the voltage-clamp mode with a first patch pipette, we thus investigated whether touching nearby astrocytes with a second patch pipette resulted in a depolarization of neurons. After astrocyte stimulation ($n = 11$), we never observed any slow depolarizing current in recorded neurons ($n = 7$).

Astrocyte-mediated dilation depends on a COX product

We next aimed to identify the agents involved in astrocyte-mediated vasodilation. Given that activation of mGluRs in cultured astrocytes triggers a Ca^{2+}-dependent release of prostaglandins (PGs)[15], molecules such as the vasodilator PGE_2 are good candidates. In slices preincubated with aspirin to inhibit the PG-forming enzyme cyclooxygenase (COX), the direct stimulation of astrocytes elicited a small dilation in only two of eleven arterioles tested (**Fig. 5a** and **b**). Furthermore, after COX inhibition, the dilating effect of *t*-ACPD was observed in only 35.7% of the arterioles examined (5 of 14 versus 32 of 41 in controls, $P = 0.0048$; mean dilation, 12.6 ± 3.03%; **Fig. 5b**). Most importantly, in the presence of aspirin, afferent stimulation was effective in only 10% (1 of 10) arterioles, as compared to 50% in controls (8 of 16, $P = 0.0418$; **Fig. 5b**). Together, these results clearly indicate that the control exerted by neuron-to-astrocyte signaling on cerebral microcirculation is predominantly dependent on the action of a COX product.

In vivo effects of mGluR antagonists

The relevance of these data in the phenomenon of functional hyperemia was investigated in rats that were subjected to electrical forepaw stimulation. The mGluR antagonists that inhibited the activation of astrocytes in acute brain slices pass the blood–brain barrier, and can thus be administered systemically[19,28]. Laser-Doppler flowmetry[29] showed that infusion of 0.5 mg/kg MPEP and 0.5 mg/kg LY367385 markedly altered the coupling between functional activation and blood flow during somatosensory stimulation (**Fig. 6**) without significantly affecting basal flow rate (1.3 ± 0.6%, n.s.; **Supplementary Fig. 4**). Before application of the mGluR antagonists, forepaw stimulation evoked a primary somatosensory cortical potential (SEP) of amplitude 33 ± 9 μV (mean ± s.e.m., $n = 5$) and a coupled increase of laser-Doppler flow (LDF) of 23 ± 7% (**Fig. 6c** and **d**). Flow sharply increased after the onset of stimulation with a delay of about 1 s, and after cessation of stimulation returned to baseline within less than 10 s. After the application of MPEP/LY, but not of the vehicle alone, the blood flow response was drastically reduced (**Fig. 6a**; also **Supplementary Fig. 4**). In the presence of mGluR antagonists, stimulation evoked a mean increase of the LDF signal of only 8 ± 1.8%, which represents a reduction of the blood flow response to 34.8% of control values (**Fig. 6c**; $P < 0.01$). In contrast, SEPs were of about the same amplitude (31 ± 8 μV compared with 33 ± 9 μV in controls, n.s.; **Fig. 6b** and **d**). The infusion of the mGluR antagonists did not change arterial pCO_2 (39.8 ± 1.9 mmHg before and 39 ± 3 mmHg after MPEP/LY), arterial pH (7.49 ± 0.02 before and 7.458 ± 0.03 after MPEP/LY) or blood pressure (130 ± 25 mmHg before and 132 ± 23 mmHg after MPEP/LY).

Discussion

Here we show that neuron-to-astrocyte signaling in the cerebral cortex is centrally involved in the dynamic control exerted by neurons on vascular tone.

The first clue for the involvement of astrocytes in neuronal–vascular coupling was the observation that the stimulation of neuronal afferents that triggered dilation of cortical arterioles also triggered $[Ca^{2+}]_i$ elevations in astrocyte endfeet that were in contact with arterioles. Astrocyte $[Ca^{2+}]_i$ oscillations may thus represent a neuron-dependent signaling system that allows these cells to work as bridges between neurons and blood vessels. This conclusion is further supported by the observation that $[Ca^{2+}]_i$ elevations that were triggered in astrocyte somata and endfeet by afferent stimulation were temporally correlated with arteriole dilation. In the presence of mGluR antagonists that inhibited neuronal activity-dependent $[Ca^{2+}]_i$ elevations in astrocytes, but not in neurons, neuronal activity–dependent vasodilation was also impaired. This indicates that there is a causal link between the astrocyte response to neuronal activity and arteriole dilation. Accordingly, the astrocyte $[Ca^{2+}]_i$ elevations elicited by the mGluR agonist *t*-ACPD triggered dilation of arterioles, even when *t*-ACPD was applied in the presence of TTX and TeNT (blockers of neuronal activity and neurotransmitter release, respectively). In slices preincubated with L-NAME and those exposed to the NMDAR antagonist D-AP5, the efficacy of afferent stimula-

© 2003 Nature Publishing Group http://www.nature.com/natureneuroscience

tion and *t*-ACPD in triggering vasodilation was not noticeably affected. Taken together, our results support the view that in the cerebral cortex, NO acts more as a permissive or modulatory factor than as a mediator of vasodilation[30,31]. This stands in contrast to the cerebellum, where the crucial role of NO in neurovascular coupling is well established[32,33].

Direct evidence for the ability of astrocytes to control arteriole tone was obtained in the experiments in which we directly and selectively stimulated individual astrocytes with a patch pipette and observed a dilation of the arteriole in closest proximity to the stimulated cell. These results also suggest that astrocytes can exert their action on arterioles without the contribution of factors that neurons may release upon activation. Astrocytes may act directly on smooth muscle cells or indirectly through endothelial cells which, in turn, may release vasodilating products. This remains to be clarified.

Several lines of evidence support the conclusion that astrocyte-mediated vasodilation depends mainly on the action of COX products: (i) PGs (in particular PGE_2) are released from astrocytes after mGluR activation[15], and this release is regulated by $[Ca^{2+}]_i$ oscillations (M.Z. *et al.*, unpub. data), (ii) *in vivo* experiments show that COX inhibition[34,35] or COX deletion[36] reduces activity-dependent increases in CBF and (iii) COX inhibitors significantly reduced vasodilation that was triggered by afferent stimulation, *t*-ACPD application or direct astrocyte activation. These results provide evidence for a major role for a COX product such as PGE_2 in astrocyte-mediated vasodilation, although additional factors released either from astrocytes and/or from neurons may also contribute.

Results obtained in adult rats *in vivo* corroborated the role of astrocyte activation in the mechanism that couples synaptic activity to CBF. After systemic injection of the same mGluR antagonists that, in brain slices, blocked the activation of astrocytes by neuronal activity, the CBF response, but not the evoked potential, triggered in the somatosensory cortex by contralateral forepaw stimulation was significantly reduced. The reduction in the CBF response can not be ascribed to changes in arterial pCO_2, arterial pH or blood pressure, as they did not change after MPEP/LY. It was also unrelated to arousal effects because in chloralose-anaesthetized rats, the blood flow response was observed only in the primary somatosensory cortex as a specific consequence of electrical forepaw stimulation[37]. The inhibition of functional hyperemia by MPEP/LY, therefore, is unrelated to nonspecific alterations in the intensity of neuronal activation or to the general physiological state. This is in full agreement with the unchanged amplitude of stimulus-evoked $[Ca^{2+}]_i$ elevations in neurons from cortical slices in the presence of MPEP/LY (**Fig. 2a** and **b**).

Admittedly, the kinetics of the response of cerebral blood vessels to neuronal activity in our slice preparations are different from *in vivo* response kinetics. Indeed, the response *in vivo* normally occurs 1–2 s after the onset of stimulation and rapidly recovers to baseline, whereas the vasodilatory response to neuronal stimulation in slices occurred, on average, 32.8 s after the onset of stimulation. In only one case did we observe a vasodilatory response 1 s after the onset of stimulation. The response in slices is thus delayed and, in general, more persistent than the response *in vivo*. A plausible explanation for this difference is that in slice preparations, a relevant part of synaptic connections is lost. The slower activation of the vessel response may thus be due to a lower excitatory drive that can be activated by the extracellular electrode in slices, as compared to *in vivo* conditions. Furthermore, the absence of intraluminal flow and pressure in slices decreases myogenic tone, which probably hampers the full responsiveness of the arteriole and limits the recovery of the arteriole tone after stimulation offset. Another possible explanation for the slow recovery is that the lack of intraluminal flow delays the removal of the dilating agents and thus results in their prolonged action. Clearly, the complexity of the mechanism underlining functional hypermia can not be solved solely in *in vitro* experiments. Our slice preparation, however, represents a model system that allowed us to test our hypothesis on the role of astrocytes in the control of cerebral microcirculation and is the prerequisite for *in vivo* experiments.

Over the past decade, neuron-to-glia communication has been identified as a signaling system that has important physiological implications[38–40]. Astrocytes can sense neuronal activity and provide a feedback mechanism that, through the release of glutamate, profoundly affects the communication between neurons[12,27,41,42]. By showing that astrocytes are involved in neuronal activity–dependent changes in neocortical microcirculation, we posit a new role for astrocytes in the brain. Our results may represent a clue for understanding the mechanism underlying cerebrovascular deficiencies occurring in numerous CNS pathologies such as Alzheimer's disease[43] and may also contribute to the interpretation of data from modern functional brain imaging techniques[44]. In fact, functional magnetic resonance imaging (fMRI) is based on the blood oxygenation level–dependent (BOLD) increase in signal intensity, which results from the rise of oxygen partial pressure in the activated brain region[45]. This hyperoxic response is characterized by a dissociation between the marked increase of blood flow and glucose use on one hand, and the much smaller increase in oxygen consumption on the other[46]. It has been proposed that the disproportional increase in glucose use is due to the stimulation of anaerobic glycolysis in astrocytes, which serves as a fast energy source for the astrocytic uptake of glutamate and its enzymatic conversion to glutamine and provides lactate as a preferred metabolic substrate for neurons[47]. The glutamate-dependent astrocytic control of blood flow reported here provides an attractive explanation for the fact that the increase of blood flow is coupled to the high (astrocytic) increase in glucose use and not to the low (neuronal) increase in oxygen consumption. The MR-visible hyperoxygenation of activated tissue may thus be a well-matched adjustment to astrocytic glucose use rather than an overcompensation for the increase in neuronal oxygen consumption. As the former depends on the total amount of synaptically released glutamate, the BOLD response is, in fact, a robust indicator of functional activation.

On the basis of our results, we propose the following model: (i) during high synaptic activity, glutamate released from axonal terminals diffuses to astrocyte membranes located at the border of the synaptic cleft, (ii) the ensuing activation of mGluRs triggers $[Ca^{2+}]_i$ oscillations on astrocyte processes that spread to the endfeet that are in contact with arterioles and (iii) these $[Ca^{2+}]_i$ elevations regulate the release of a vasoactive agent, most likely a COX product, from astrocytes (presumably from their endfeet) that leads to blood flow increase. While our data do not exclude the possibility that multiple factors and signaling pathways—including the direct innervation of vessels—contribute to functional hyperemia, they show that the activation of astrocytes is centrally involved in this process.

Methods

Slice preparation and arteriole analysis. All experimental procedures were in strict accordance with the Italian and EU regulations on animal welfare, and were authorized by the Italian Ministry of Health. Trans-

© 2003 Nature Publishing Group http://www.nature.com/natureneuroscience

verse cortical slices from 9–15 day old Wistar rats were obtained as previously described[12,48]. Slices were continuously perfused with an external solution containing NaCl (120 mM), KCl (3.2 mM), KH_2PO_4 (1 mM), $NaHCO_3$ (26 mM), $MgCl_2$ (1 mM), $CaCl_2$ (2 mM) and glucose (2.8 mM); pH 7.4 with 5% CO_2/ 95% O_2 at 33 °C. Blood vessels were visualized with an upright Axioskop microscope equipped with differential interference contrast (DIC) and a CCD camera (COHU Inc., San Diego, California). We selected vessels from layers 2–5 that: (i) showed structures reminiscent of vascular myocytes, (ii) had a discernible luminal diameter of 5–20 μm and (iii) could be controlled for their integrity for a length of 100–150 μm. Images of vascular responses were acquired with Scion Image software (Frederick, Massachusetts). To measure the diameter, we compared off-line images acquired at the same focal plane from 1–4 sectors (length 15–50 μm). Intraluminal diameters for each experimental time point were derived as an average of 6–25 measurements taken every 2–4 μm along the sector (**Fig. 1a**). Baseline diameter values were obtained during a 20–40 min equilibration period, and only vessels with a stable diameter were considered (mean vessel diameter, 9.7 ± 0.32 μm; $n = 205$). In the different experiments, the number of arterioles studied corresponds to the number of slices used (only one arteriole per slice was examined). To obtain a threshold for considering an increase in the diameter as a significant dilation, in all arterioles we set the first diameter value after the equilibration period to 100 and calculated its average relative change after a further period of 10–20 min. The obtained value was 99.8 ± 2.6% (mean diameter ± s.d.). Only a diameter increase of >5.2% (twice the value of the s.d.) after application of the dilating stimulus was considered to be a significant dilation.

Stimulation protocol. Stimulation of neuronal afferents was performed by applying high-frequency (100 Hz) trains of 200 ms at 0.2 Hz for 4 min or a pulse of 200 μs at 20 Hz for 1 min with a concentric bipolar electrode (1–9 mA; inner pole wire diameter, 25 μm; FHS, Bowdoinham, Maine) placed 300–500 μm from the recorded arteriole. To control for a possible direct stimulation of vascular myocytes, by whole-cell patch clamp recordings we routinely ascertained that a neuron located between the electrode and the vessel under study did not show a direct depolarization and action potential firing. We also verified that a very high-intensity stimulus, in addition to triggering the direct depolarization and firing of the neuron, always resulted in a powerful vasoconstriction ($n = 4$). Standard procedures for pipette preparation and patch clamp recordings were used. The recording pipette contained: K-gluconate (145 mM), $MgCl_2$ (1 mM), Na-ATP (4 mM), EGTA (0 or 5 mM) and HEPES (10 mM), pH 7.2. Electrophysiological data were obtained using an Axopatch 200B (Axon Instruments, Foster City, California) filtered at 1–5 kHz and analyzed using pClamp8 software (Axon Instruments). Individual astrocytes were stimulated in current-clamp mode with a Lucifer yellow–filled (0.4–0.8%) patch pipette using single current pulses (500 ms at 0.25 Hz, amplitude 100–3,000 pA) that depolarize cells to about +50 mV. In slices loaded with either Fluo-3 or Oregon green, a mechanical stimulus applied with a patch pipette to the astrocyte was confirmed to rapidly trigger $[Ca^{2+}]_i$ elevations ($n = 4$). Astrocytes were distinguished from neurons by (i) small and round cell soma (diameter range, 6–10 μm) lacking optically apparent large processes, (ii) highly negative resting potentials (–79 ± 2.1 mV, mean ± s.e.m.; $n = 33$) and (iii) incapacity to discharge action potentials upon application of depolarizing current pulses. Stimulation of astrocytes was performed also with *t*-ACPD either in the absence or in the presence of drugs: TTX (1 μM), TeNT (100 μg/ml), the COX inhibitors indomethacin (5 μM) or aspirin (50 μM), and L-NAME (100 μM). Before the application of the various stimuli, L-NAME and COX inhibitors were applied in the perfusate for 40 min, MPEP, LY367385 and D-AP5 for 5 min. Preincubation with TeNT was performed at 37 °C for 50 min. MPEP, LY367385, *t*-ACPD and TTX were purchased from Tocris Cookson (Bristol, UK); L-NAME and COX inhibitors were from Sigma (St. Louis, Missouri); and PGE_2, the prostacyclin PGI_2 and $PGF_{2\alpha}$ were from Biomol (Plymouth, Pennsylvania).

Confocal microscope experiments. Slices were incubated in 20 μM Indo-1/AM (the acetoxymethyl derivate of Indo-1, Molecular Probes, Eugene, Oregon), 200 μM sulfinpyrazone and 0.04% pluronic at 37 °C for 1 h. Digital fluorescence microscopy was performed using a Nikon inverted microscope (Diaphot 300) equipped with a 40× water immersion objective (NA = 1.1) and connected to a real-time confocal system (Nikon RCM8000). The ratio of the intensity of the light emitted at two wavelengths (405/485R) was displayed as a pseudocolor scale. Neurons and astrocytes were distinguished on the basis of the distinct kinetics of their response to a high K^+ stimulation, as previously reported[12]. Owing to the modest loading of smooth muscle and endothelial cells with Indo-1, the luminal diameter could not be measured in a reliable manner. Dilation was, therefore, hardly detectable in the experiments in which we followed $[Ca^{2+}]_i$ changes in astrocyte endfeet outlining the external profile of arterioles. This external profile did not change significantly after dilating or constrictive stimuli. Even in a few experiments in which endothelial and muscle cells showed a relatively good loading, the focal plane that would allow us to measure the luminal diameter of the arteriole was different from that of the astrocyte endfeet. Shifting from one focal plane to the other during acquisition was not feasible.

***In vivo* experiments.** Five adult normothermic rats (320–410 g) were anaesthetized with 1.5% halothane, immobilized with 0.2 mg/kg/h pancuronium and mechanically ventilated with oxygen-enriched air throughout the experiments. Blood gases were monitored repeatedly and kept in the physiological range; body temperature was kept constant at 37 °C using a feedback-controlled heating system. After completion of surgery, halothane supply was discontinued and anesthesia was maintained by hourly intravenous injections of 20 mg/kg alpha-chloralose. Somatosensory stimulation was carried out by applying trains of electrical pulses to the right forepaw (stimulation frequency 2 Hz, pulse length 0.3 ms, intensity 1 mA). Laser-Doppler flow (LDF) and primary evoked potentials were recorded from the contralateral somatosensory cortex[29]. The specificity of the response was confirmed by testing the absence of a flow increase during stimulation of the left (ipsilateral) forepaw. The evoked potentials and the integrated LDF responses were averaged (10 stimulation trains of 30 s duration each, separated by 30 s recovery) and compared before and 15–20 min after intravenous infusion of 0.5 mg/kg MPEP and 0.5 mg/kg LY367385.

Statistics. Values were expressed as mean ± s.e.m. and tested for statistical differences ($P < 0.05$) using Student's *t*-test (n.s., non-significant). The statistical significance of the difference in the number of responsive arterioles under the various experimental conditions was evaluated by Fisher's exact test.

Note: Supplementary information is available on the Nature Neuroscience website.

Acknowledgments

We thank P. Magalhães for comments on the manuscript and C. Montecucco for the supply of purified tetanus neurotoxin. M.C.A. was supported by the Human Frontier Science Program Organization (HFSPO). This work was supported by grants from the Armenise Harvard University Foundation, the Italian University and Health Ministries, the Italian Association for Cancer Research (AIRC), the Human Frontier Science Program (RG520/95), the ST/Murst 'Neuroscienze' to G.C., Telethon-Italy (845 and 850 to T.P.; 1095 to G.C.), and the European Community (QLG3-CT-2000-00934).

Competing interests statement

The authors declare that they have no competing financial interests.

RECEIVED 23 SEPTEMBER; ACCEPTED 5 NOVEMBER 2002

1. Roy, C.S. & Sherrington, C. On the regulation of the blood supply of the brain. *J. Physiol.* **11**, 85–108 (1890).
2. Reinhard, J.F. Jr., Liebmann, J.E., Schlosberg, A.J. & Moskowitz, M.A. Serotonin neurons project to small blood vessels in the brain. *Science* **206**, 85–87 (1979).
3. Vaucher, E. & Hamel, E. Cholinergic basal forebrain neurons project to cortical microvessels in the rat: electron microscopic study with anterogradely transported Phaseolus vulgaris leucoagglutinin and choline acetyltransferase immunocytochemistry. *J. Neurosci.* **15**, 7427–7441 (1995).

© 2003 Nature Publishing Group http://www.nature.com/natureneuroscience

4. Krimer, L.S., Muly, E.C., Williams, G.V. & Goldman-Rakic, P.S. Dopaminergic regulation of cerebral cortical microcirculation. *Nat. Neurosci.* **1**, 286–289 (1998).
5. Paspalas, C.D. & Papadopoulos, G.C. Ultrastructural evidence for combined action of noradrenaline and vasoactive intestinal polypeptide upon neurons, astrocytes, and blood vessels of the rat cerebral cortex. *Brain Res. Bull.* **45**, 247–259 (1998).
6. Yang, G., Huard, J.M., Beitz, A.J., Ross, M.E. & Iadecola, C. Stellate neurons mediate functional hyperemia in the cerebellar molecular layer. *J. Neurosci.* **20**, 6968–6973 (2000).
7. Faraci, F.M. & Heistad, D.D. Regulation of the cerebral circulation: role of endothelium and potassium channels. *Physiol. Rev.* **78**, 53–97 (1998).
8. Golgi, C. Sulla fina anatomia degli organi centrali del sistema nervoso. *Riv. Sper. Fremiat. Med. Leg. Alienazioni Ment.* **11**, 72–123 (1885).
9. Peters, A., Palay, S.L. & Webster, H.d.F. in *The Fine Structure of the Central Nervous System: Neurons and Their Supportive Cells* (ed. Press, O.U.) 276–295 (Oxford Univ. Press, New York, 1991).
10. Ventura, R. & Harris, K.M. Three-dimensional relationships between hippocampal synapses and astrocytes. *J. Neurosci.* **19**, 6897–6906 (1999).
11. Porter, J.T. & McCarthy, K.D. Hippocampal astrocytes *in situ* respond to glutamate released from synaptic terminals. *J. Neurosci.* **16**, 5073–5081 (1996).
12. Pasti, L., Volterra, A., Pozzan, T. & Carmignoto, G. Intracellular calcium oscillations in astrocytes: a highly plastic, bidirectional form of communication between neurons and astrocytes *in situ*. *J. Neurosci.* **17**, 7817–7830 (1997).
13. Kang, J., Jiang, L., Goldman, S.A. & Nedergaard, M. Astrocyte-mediated potentiation of inhibitory synaptic transmission. *Nat. Neurosci.* **1**, 683–692 (1998).
14. Alkayed, N.J. *et al.* Role of P-450 arachidonic acid epoxygenase in the response of cerebral blood flow to glutamate in rats. *Stroke* **28**, 1066–1072 (1997).
15. Bezzi, P. *et al.* Prostaglandins stimulate calcium-dependent glutamate release in astrocytes. *Nature* **391**, 281–285 (1998).
16. Sagher, O. *et al.* Live computerized videomicroscopy of cerebral microvessels in brain slices. *J. Cereb. Blood Flow Metab.* **13**, 676–682 (1993).
17. Fergus, A., Jin, Y., Thai, Q.A., Kassell, N.F. & Lee, K.S. Vasodilatory actions of calcitonin gene-related peptide and nitric oxide in parenchymal microvessels of the rat hippocampus. *Brain Res.* **694**, 78–84 (1995).
18. Farber, N.E. *et al.* Region-specific and agent-specific dilation of intracerebral microvessels by volatile anesthetics in rat brain slices. *Anesthesiology* **87**, 1191–1198 (1997).
19. Gasparini, F. *et al.* 2-Methyl-6-(phenylethynyl)-pyridine (MPEP), a potent, selective and systemically active mGlu5 receptor antagonist. *Neuropharmacology* **38**, 1493–1503 (1999).
20. Garthwaite, J., Charles, S.L. & Chess-Williams, R. Endothelium-derived relaxing factor release on activation of NMDA receptors suggests role as intercellular messenger in the brain. *Nature* **336**, 385–388 (1988).
21. Garthwaite, J. Glutamate, nitric oxide and cell-cell signaling in the nervous system. *Trends Neurosci.* **14**, 60–67 (1991).
22. Iadecola, C. Regulation of the cerebral microcirculation during neural activity: is nitric oxide the missing link? *Trends Neurosci.* **16**, 206–214 (1993).
23. Fergus, A. & Lee, K.S. Regulation of cerebral microvessels by glutamatergic mechanisms. *Brain Res.* **754**, 35–45 (1997).
24. Fagni, L., Chavis, P., Ango, F. & Bockaert, J. Complex interactions between mGluRs, intracellular Ca2+ stores and ion channels in neurons. *Trends Neurosci.* **23**, 80–88 (2000).
25. Skeberdis, V.A. *et al.* mGluR1-mediated potentiation of NMDA receptors involves a rise in intracellular calcium and activation of protein kinase C. *Neuropharmacology* **40**, 856–865 (2001).
26. Schiavo, G. *et al.* Tetanus and botulinum-B neurotoxins block neurotransmitter release by proteolytic cleavage of synaptobrevin. *Nature* **359**, 832–835 (1992).
27. Parpura, V. *et al.* Glutamate-mediated astrocyte-neuron signalling. *Nature* **369**, 744–747 (1994).
28. Monn, J.A. *et al.* Synthesis, pharmacological characterization, and molecular modeling of heterobicyclic amino acids related to (+)-2-aminobicyclo[3.1.0] hexane- 2,6-dicarboxylic acid (LY354740): identification of two new potent, selective, and systemically active agonists for group II metabotropic glutamate receptors. *J. Med. Chem.* **42**, 1027–1040 (1999).
29. Schmitz, B., Bottiger, B.W. & Hossmann, K.A. Functional activation of cerebral blood flow after cardiac arrest in rat. *J. Cereb. Blood Flow Metab.* **17**, 1202–1209 (1997).
30. White, R.P., Deane, C., Vallance, P. & Markus, H.S. Nitric oxide synthase inhibition in humans reduces cerebral blood flow but not the hyperemic response to hypercapnia. *Stroke* **29**, 467–472 (1998).
31. Lindauer, U., Megow, D., Matsuda, H. & Dirnagl, U. Nitric oxide: a modulator, but not a mediator, of neurovascular coupling in rat somatosensory cortex. *Am. J. Physiol.* **277**, 799–811 (1999).
32. Iadecola, C., Zhang, F. & Xu, X. Role of nitric oxide synthase-containing vascular nerves in cerebrovasodilation elicited from cerebellum. *Am. J. Physiol.* **264**, 738–746 (1993).
33. Yang, G., Chen, G., Ebner, T.J. & Iadecola, C. Nitric oxide is the predominant mediator of cerebellar hyperemia during somatosensory activation in rats. *Am. J. Physiol.* **277**, 1760–1770 (1999).
34. Golanov, E.V. & Reis, D.J. Nitric oxide and prostanoids participate in cerebral vasodilation elicited by electrical stimulation of the rostral ventrolateral medulla. *J. Cereb. Blood Flow Metab.* **14**, 492–502 (1994).
35. Bakalova, R., Matsuura, T. & Kanno, I. The cyclooxygenase inhibitors indomethacin and Rofecoxib reduce regional cerebral blood flow evoked by somatosensory stimulation in rats. *Exp. Biol. Med.* **227**, 465–473 (2002).
36. Niwa, K., Araki, E., Morham, S.G., Ross, M.E. & Iadecola, C. Cyclooxygenase-2 contributes to functional hyperemia in whisker-barrel cortex. *J. Neurosci.* **20**, 763–770 (2000).
37. Brinker, G. *et al.* Simultaneous recording of evoked potentials and T2*-weighted MR images during somatosensory stimulation of rat. *Magn. Reson. Med.* **41**, 469–473 (1999).
38. Carmignoto, G. Reciprocal communication systems between astrocytes and neurones. *Prog. Neurobiol.* **62**, 561–581 (2000).
39. Haydon, P.G. GLIA: listening and talking to the synapse. *Nat. Rev. Neurosci.* **2**, 185–193 (2001).
40. Robitaille, R. Modulation of synaptic efficacy and synaptic depression by glial cells at the frog neuromuscular junction. *Neuron* **21**, 847–855 (1998).
41. Araque, A., Sanzgiri, R.P., Parpura, V. & Haydon, P.G. Calcium elevation in astrocytes causes an NMDA receptor-dependent increase in the frequency of miniature synaptic currents in cultured hippocampal neurons. *J. Neurosci.* **18**, 6822–6829 (1998).
42. Parri, H.R., Gould, T.M. & Crunelli, V. Spontaneous astrocytic Ca^{2+} oscillations *in situ* drive NMDAR-mediated neuronal excitation. *Nat. Neurosci.* **4**, 803–812 (2001).
43. de la Torre, J.C. Alzheimer disease as a vascular disorder: nosological evidence. *Stroke* **33**, 1152–1162 (2002).
44. Raichle, M.E. Cognitive neuroscience. Bold insights. *Nature* **412**, 128–130 (2001).
45. Fox, P.T., Raichle, M.E., Mintun, M.A. & Dence, C. Nonoxidative glucose consumption during focal physiologic neural activity. *Science* **241**, 462–464 (1988).
46. Logothetis, N.K., Pauls, J., Augath, M., Trinath, T. & Oeltermann, A. Neurophysiological investigation of the basis of the fMRI signal. *Nature* **412**, 150–157 (2001).
47. Pellerin, L. & Magistretti, P.J. Glutamate uptake into astrocytes stimulates aerobic glycolysis: a mechanism coupling neuronal activity to glucose utilization. *Proc. Natl. Acad. Sci. USA* **91**, 10625–10629 (1994).
48. Carmignoto, G. & Vicini, S. Activity-dependent decrease in NMDA receptor responses during development of the visual cortex. *Science* **258**, 1007–1011 (1992).